JOURNAL OF MATERIALS SCIENCE 33 (1998) 2067–2072

Charge transport and structural morphology of HCl-doped polyaniline

R. SINGH, V. ARORA, R. P. TANDON, S. CHANDRA
National Physical Laboratory, Dr K. S. Krishnan Marg, New Delhi 110012, India
A. MANSINGH
Department of Physics and Astrophysics, University of Delhi, Delhi 110007, India
E-mail: ramadhar@csnpl.ren.nic.in

The d.c. and a.c. (100 Hz–1 MHz) conductivities of HCl-doped polyaniline have been measured in the temperature range 77–300 K. At 77 K, the a.c. conductivity data, $\sigma(\omega)$, can be described by the relation $\sigma(\omega) = A\omega^s$, where the parameter s lies close to unity and decreases with increase in the doping level. The ratio of measured a.c. to d.c. conductivity shows dispersion at 77 K, which decreases with increase in the doping level. This decrease is found to be sharp around pH $\sim$ 3.0. In the temperature range 77–150 K, the observed d.c. conductivity data can be described by Mott's three dimensional variable range hopping (VRH) model. Scanning electron microscopy studies reveal a sharp change in structural morphology of HCl-doped polyaniline at a pH $\sim$ 3.0. A strikingly remarkable structural morphology has been observed in the form of a channel at this pH value. This change is accompanied by a rapid increase in d.c. conductivity, dielectric constant, along with sharp changes in structural morphology, which indicates the existence of a doping-induced structural conductivity correlation in this system. © *1998 Chapman & Hall*

1. Introduction

Polyaniline (PAN) has become one of the most technologically important polymeric materials [1] due to its unique processibility together with relatively inexpensive monomer and high yield of polymerization. PAN is fast replacing the conventional materials because of its fascinating electrical properties, such as variation of its electrical conductivity both by the process of protonation and oxidation. It is well established that HCl-doped PAN exhibits metal–insulator transition and the nature of the charge transport has remained the subject of many studies during recent years [2–10]. The nearly linear dependence of Pauli susceptibility on protonation level, and of the Seebeck coefficients on reciprocal temperature [5, 6] provides evidence that the emeraldine salt form of PAN segregates into three-dimensional metallic islands surrounded by an amorphous region [2, 3, 5, 6, 11, 12]. Band-structure calculations [13] for protonated PAN reveal a highly asymmetric valence and conduction bands with only a half-occupied polaron band deep in the gap as opposed to the usual two bands in a normal conducting polymer. Very few models for charge transport [3, 6, 14] are available in the literature on lightly doped samples of PAN as the prime interest of the researchers in this field was to enance conductivity by doping.

The present paper is a report of the measurements of a.c. conductivity (100 Hz–1 MHz) and d.c. conductivity on lightly doped samples of HCl-doped polyaniline. An attempt has been made to correlate the structural morphology to conductivity and dielectric data. The d.c. conductivity data have been analysed in the light of existing theoretical models.

2. Experimental procedure

The emeraldine salt (ES) form of PAN was prepared by chemical polymerization of aniline and HCl at 270K to which ammonium persulphate $(NH_4)_2S_2O_8$ was added. After dedoping ES with ammonia solution for 24 h, a violet–brown precipitate called emeraldine base (EB) was obtained. This EB was extracted with tetrahydrofuran in order to remove oligomers. EB was then treated with different concentrations of HCl to achieve a constant pH value. The resulting samples with various pH values have been denoted Al–A8 (Table I). Pellets of uniform thickness were pressed under a pressure of 15×10^3 p.s.i. (10^3 p.s.i. = 6.89 N mm^{-2}). Scanning electron micrographs of these samples were taken using a scanning electron microscope, Jeol JSM 840. Electron diffraction patterns (EDP) were taken using a transmission electron microscope, Jeol JEM 2000 EX. The samples for TEM investigation were prepared by placing very finely ground powder on grids. Gold electrodes were vacuum deposited on both sides of these samples making an Au–PAN–Au configuration. Before each

TABLE I Variation of conductivity with pH

No.	Sample	pH	$\sigma_{d.c.}(\Omega^{-1}\,cm^{-1})$
1	A1	>7 (EB)	2.7×10^{-11}
2	A2	4.25	2.5×10^{-8}
3	A3	4.15	8.0×10^{-8}
4	A4	4.00	2.0×10^{-6}
5	A5	3.50	1.0×10^{-4}
6	A6	3.00	5.0×10^{-4}
7	A7	2.35	9.8×10^{-3}
8	A8	0 (ES)	0.8×10^{1}

measurement, samples were again dried in vacuum to eliminate the effect of absorbed water. The d.c. conductivity of samples A3, A4, A5 and A6 was measured using a Keithley 617 electrometer and Keithley 2000 DMM in the temperature range 77–300 K. The a.c. conductivity of different samples of PAN was measured by using a HP 4192A LF impedance analyser in the frequency range 100 Hz–1 MHz and in the temperature range 77–300 K. The dielectric constant, (ε'), at a frequency of 1 kHz was also measured for these samples.

3. Results and discussion

The doping of PAN with HCl has been found to cause drastic changes in its electrical and structural properties. Fig. 1 shows the measured d.c. conductivity $\sigma_{d.c.}$ and dielectric constant, ε', as a function of pH. It is evident from this figure that the d.c.

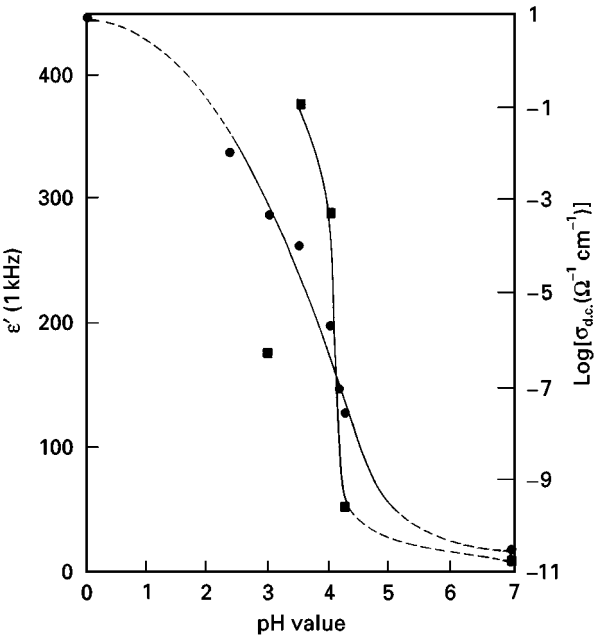

Figure 1 The (●) d.c. conductivity ($\log \sigma_{d.c.}$) and (■) dielectric constant (1 kHz) plotted as a function of pH, at 300K.

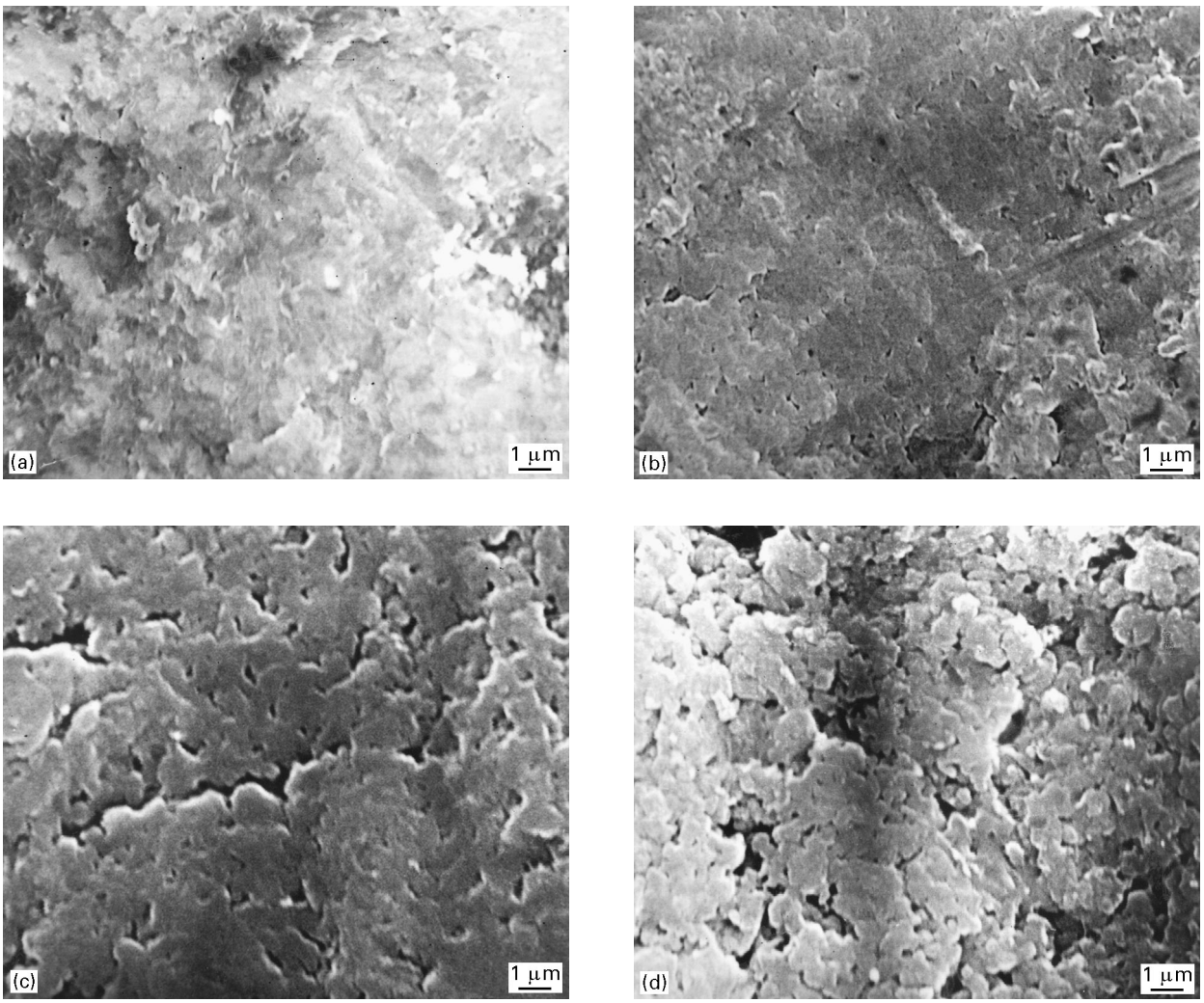

Figure 2 Scanning electron micrographs taken on undoped and HCl-doped polyaniline: (a) EB, (b) pH = 3.5, (c) pH = 3.0, (d) ES.

conductivity increases rapidly in the pH range 3.50–4.25, which seems to have correlation with its structural morphology, and will be discussed subsequently.

Fig. 2 shows scanning electron micrographs of these samples. It is evident from Fig. 2 that for the EB form of PAN, only lumps of the material can be seen (Fig. 2a). At pH $\sim$ 3.5, channel formation can be seen at its preliminary stage (Fig. 2b). It is quite interesting to note that with its very inception, the conductivity is found to increase rapidly. This leads to an irregular channel formation [15]. This structure at pH value $\sim$ 3.0 (Fig. 2c) can be classified as an inhomogeneous media consisting of a conductor and an insulator. It can also be considered as a structure with a continuous conducting channel or linkage or chain in an insulating matrix. It is found to be very similar to that of the blood vessel network [16] in the human body. Once these disordered continuous linkages are formed in the insulating matrix, the conductivity has a tendency to saturate. That is why, the d.c. conductivity is found to be composition-dependent. Further advancement in the channel formation is observed with increase in the doping level.

An increase in dielectric constant is observed with an increase in the doping level (Fig. 1). This increase is found to be very sharp when the d.c. conductivity increases rapidly and channel formation is observed (Fig. 2c). The ε' at pH $\sim$ 3.0 has a lower value than expected, because it attains a static value much below room temperature. These results of the a.c. conductivity measurements will be published elsewhere. These changes are likely to cause an inherent increase in crystallinity. The salt form of PAN (ES) (Fig. 2d) is found to assume a definite size and shape, showing therein some signs of crystallinity. The increase in crystallinity is also evident from the electron diffraction patterns (EDP) of EB and ES forms of PAN (Fig. 3). It is evident from Fig. 3a that this material (EB) is predominantly amorphous in nature, whereas ES shows a semi-crystalline structure (Fig. 3b). A direct correlation of the dielectric constant and crystallinity seems to exist here. This can be explained by the amorphous mass of EB having a low value ($\sim$6) of ε'. The dielectric constant begins to increase with increase in the doping level as soon as the microcrystallites start to become embedded in the amorphous matrix at higher doping level. This is found to be consistent with the metallic island concept for highly conducting PAN [12]. Fig. 3b also gives evidence of microcrystallites embedded in an amorphous matrix, while Fig. 3a does not reveal such a structure.

There are few reports available on the crucial pH range when the transformation of the PAN lattice takes place [17, 18]. Spectroscopic studies [18] on polyaniline have shown that sharp changes in the spectra are observed in the pH range 3–4. In the present investigation, the d.c. conductivity and dielectric constant increase sharply in the pH range 3.50–4.25. The increase in conductivity is also associated with a decrease in activation energy, E_A.

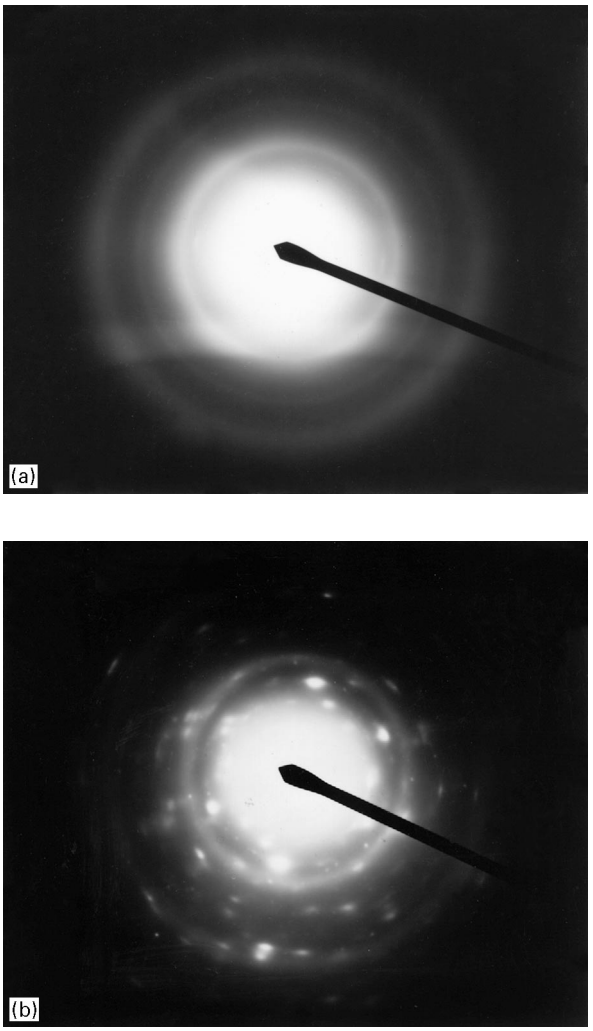

Figure 3 Electron diffraction patterns taken on (a) EB, and (b) ES forms of PAN.

The activation energy for various samples has been calculated from the slopes of log $\sigma_{d.c.}$ versus $1000/T$ plot (Fig. 4a) and are given in Table II. Fig. 5 shows the activation energy plotted as a function of doping level. This figure also shows a sharp decrease in activation energy, E_A, in a particular pH range. This also suggests a composition-dependent conductivity in this system.

The $\sigma_m/\sigma_{d.c.}$ ratio of different samples of PAN has been plotted as a function of pH in Fig. 6. It shows evidence of dispersion at 77 K which decreases with increase in the doping level. The samples having a higher doping level give higher conductivity, due to semi-quinone radical cations formed by hydrogen-bonding between the neighbouring polymers [19]. Here, the new states are formed between the valence and conduction band by HCl doping which are responsible for conduction, thereby decreasing the activation energy; a decrease in frequency dispersion is also observed at lower temperatures.

Fig. 4a shows the variation of d.c. conductivity of samples A3, A4, A5 and A6 as a function of reciprocal temperature in the temperature tange 77–300 K. The non-linearity of the curves cannot be accounted for within the framework of a band-conduction model [20–22]. It seems worthwhile to mention that Mott's

TABLE II Evaluation of various parameters for Samples A3, A4, A5 and A6

Parameters	A3	A4	A5	A6
1. T_0(log $\sigma_{d.c.}$ versus $T^{-1/2}$)	1.44×10^5 K	4.66×10^4 K	1.9×10^4 K	1.65×10^4 K
2. T_0(log $\sigma_{d.c.}$ versus $T^{-1/4}$)	3.42×10^9 K	3.64×10^8 K	6.43×10^7 K	3.67×10^7 K
3. n (slope)	–	11.2	6.7	6.1
4. Log T validity	–	146 K	143 K	138 K
5. $T^{-1/4}$ validity	180 K	154 K	148 K	145 K
6. S (slope)	–	0.73	0.58	0.49
7. $\sigma_{d.c.}(\Omega^{-1}\,cm^{-1})$ 77 K	1.26×10^{-13} (120 K)	1.12×10^{-11}	6.8×10^{-8}	2.5×10^{-7}
8. E_A (300 K) eV	0.282	0.230	0.185	0.160
9. E_A (77 K) eV	0.19 (120 K)	0.084	0.054	0.040

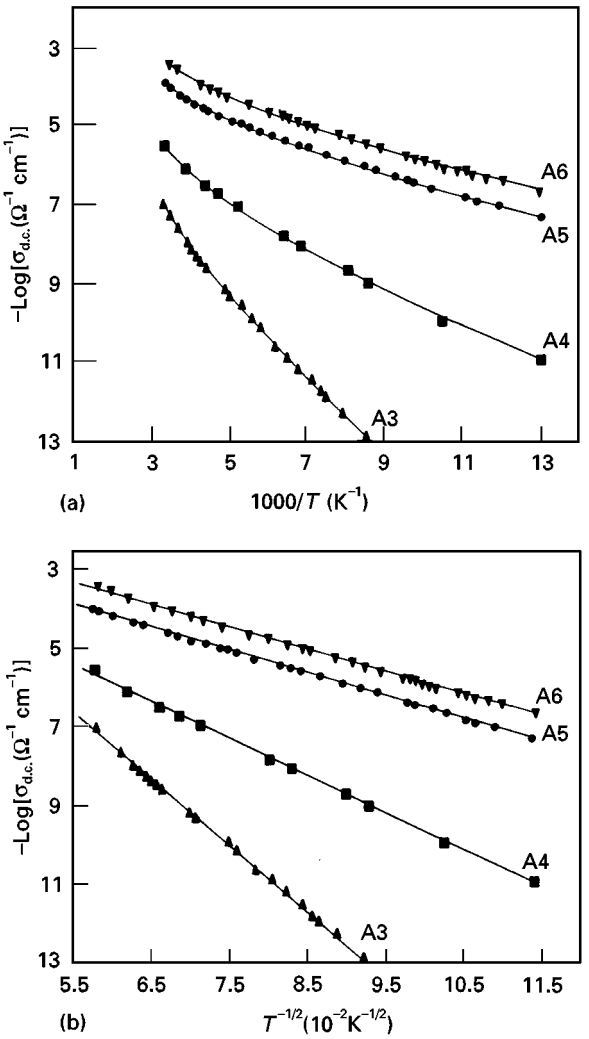

Figure 4 The d.c. conductivity (log $\sigma_{d.c.}$) plotted as a function of (a) $1000/T$ and (b) $T^{-1/2}$.

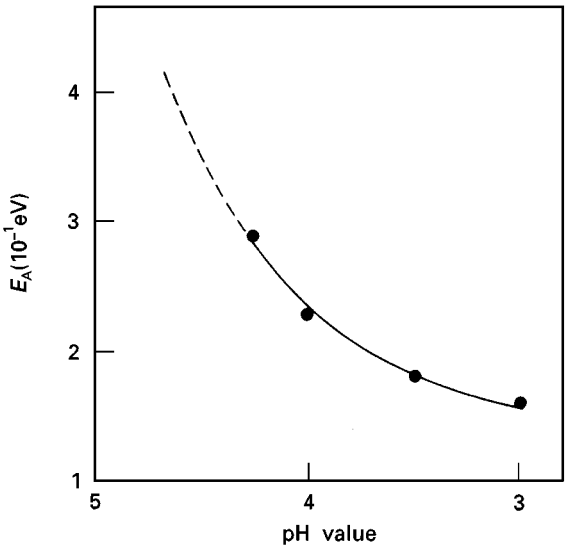

Figure 5 Activation energy, E_A, plotted as a function of pH.

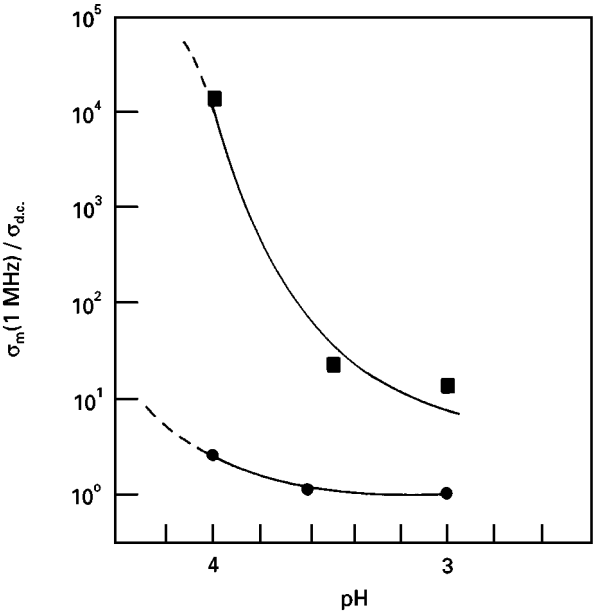

Figure 6 The measured a.c. conductivity to d.c. conductivity ratio (σ_m(1 MHz)/$\sigma_{d.c.}$) plotted as a function of pH at (■) 77 and (●) 300 K.

variable range hopping (VRH) model has been extensively applied to various amorphous inroganic semiconductors [20] over the last two decades, and has recently also been applied with varying degree of success to conducting organic systems [21–23]. Recently Reghu *et al.* [10] have shown the applicability of Mott's VRH model in polyaniline film. As a representative result, we have plotted the conductivity data of sample A5 as a function of $T^{-1/4}$, $T^{-1/2}$ and log T in Fig. 7. The results of log $\sigma_{d.c.}$ versus log T indicate that a power law behaviour [24], $\sigma_{d.c.} = AT^n$, provides a fit to the data with the value $n = 6.7$ up to 143 K. The log $\sigma_{d.c.}$ versus log T variation for these samples (Table II) show a change in the value of n and slight change in temperature after

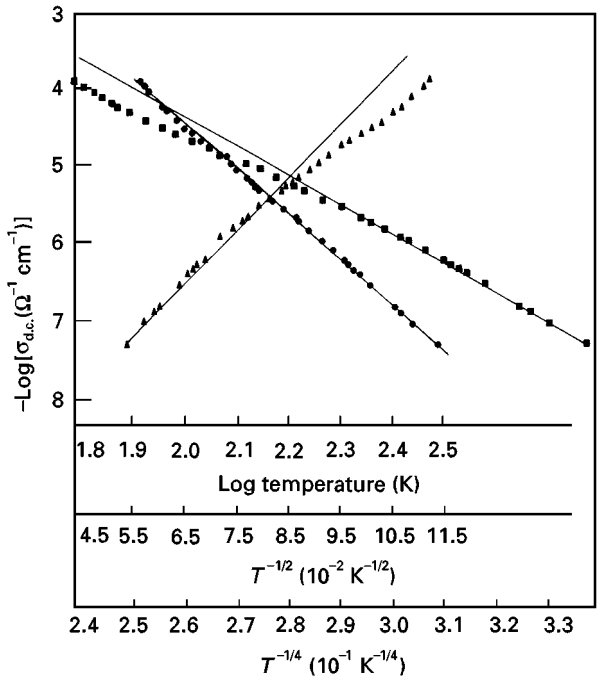

Figure 7 The d.c. conductivity (log $\sigma_{d.c.}$) plotted as a function of (●) $T^{-1/2}$, (■) $T^{-1/4}$ and (▲) log T, for sample A5.

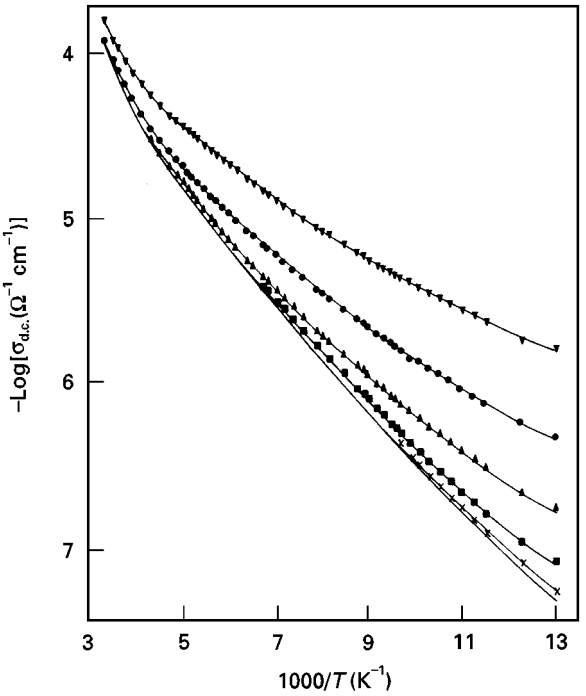

Figure 8 The measured a.c. conductivity, σ_m, along with (——) d.c. conductivity for sample A5 plotted as a function of reciprocal temperature. (×) 100 Hz, (■) 1 kHz, (▲) 10 kHz, (●) 100 kHz, (▼) 1 MHz.

which a deviation from a straight line is observed, indicating departure from Kivelson's model. However, the log $\sigma_{d.c.}$ versus $T^{-1/2}$ plot (Fig. 4b) gives a reasonable fit to the data for the whole temperature range studied. It is evident from Fig. 7 that Mott's three-dimensional VRH model gives an excellent fit to the experimental results from 77–148 K [20].

The variable range hopping conduction will give [20]

$$\sigma_{d.c.} = \sigma_0 \exp(-T_0/T)^{1/4} \quad (1)$$

where T_0 and σ_0 are constants. The slope T_0 can be calculated from the plots of log $\sigma_{d.c.}$ versus $T^{-1/4}$ and can be given as

$$T_0 = \lambda\alpha^3/k_B N(E_f) \quad (2)$$

where $\lambda \sim 18.1$ [22] is a dimensionless constant, α is the inverse rate of the fall of the wave function, k_B is Boltzmann's constant and $N(E_f)$ is the density of states at the Fermi level. The average hopping distance, R, has been estimated using the following expression

$$R = \{9/[8\pi\alpha k_B T N(E_f)]\}^{1/4} \quad (3)$$

The average hopping energy, W, can also be estimated by knowing $N(E_f)$ and R from the following relation

$$W = 3/[4\pi R^3 N(E_f)] \quad (4)$$

The value of T_0 estimated from Fig. 7 is 6.43×10^7 K. The calculated values of $N(E_f)$, R and W from the above equations are $\sim 2.45 \times 10^{18}$ cm^{-3} eV^{-1}, 10.6 nm and 0.082 eV, respectively, at 148 K after taking the value of $\alpha^{-1} = 1.1$ nm [14].

Fig. 8 shows the variation of measured a.c. conductivity, σ_m, as a function of reciprocal temperature for five fixed frequencies. The d.c. conductivity data are also included in this figure. It is evident from this figure that the temperature at which the measured a.c. conductivity equals d.c. conductivity increases with the increase in frequency. The activation energy calculated at 77 K is 0.03 eV which provides evidence [25] of electronic hopping conduction at low temperatures. The variation of $\sigma_{a.c.}$ as a function of frequency is given in Fig. 9 for samples A4, A5 and A6. At 77 K, the a.c. conductivity could be described by the relation

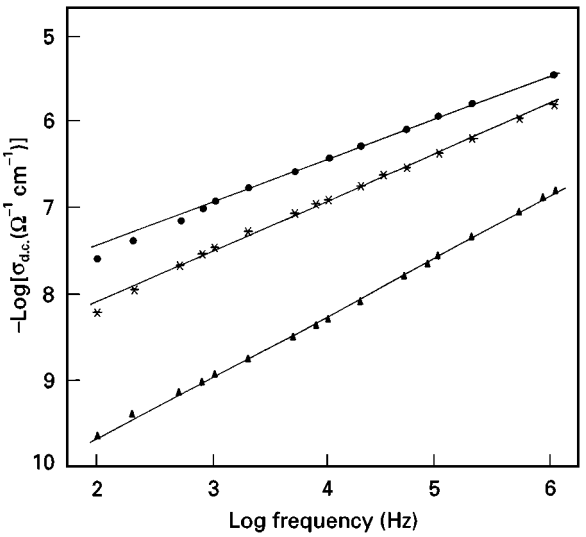

Figure 9 The variation of a.c. conductivity, $\sigma_{a.c.}$, as function of frequency. (●) Sample A6, (∗) Sample A5, (▲) Sample A4.

$$\sigma_{a.c.} = A\omega^s \quad (5)$$

where the exponent s lies close to unity which decreases with increase in doping level. (Table II). It may be noted that a large dispersion observed at low

doping level reduces to a minimum at higher doping level. This may be due to the onset of the transformation of the lattice structure of polyaniline from localization to delocalization [14, 18].

4. Conclusion

The observed d.c. conductivity data could be well explained by Mott's three-dimensional variable range hopping model at low temperatures. Sharp changes in d.c. conductivity, dielectric constant and changes in structural morphology in a particular pH range, clearly indicate the transformation of the PAN lattice.

Acknowledgements

The authors thank Professor E. S. R. Gopal, Director, National Physical Laboratory, New Delhi for his keen interest and permission to publish this work, Mr K. B. Rawat (N.P.L.) for SEM and Dr N. C. Mehra (D.U.) for performing TEM work. Mr S. U. M. Rao (N.P.L.) is thanked for many useful discussions.

References

1. Y. PHILLIPS, *Sci. Am.* **273** (1995) 75.
2. F. ZUO, M. ANGELOPOULOS, A. G. MACDIARMID and A. J. EPSTEIN, *Phys. Rev. B.* **36** (1987) 3475.
3. *Idem*, *ibid.* **39** (1989) 3570.
4. Q. LI, L. CRUZ and P. PHILLIPS, *ibid* **47** (1993) 1840.
5. Z. H. WANG, A. RAY, A. G. MACDIARMID and A. J. EPSTEIN, *ibid.* **43** (1991) 4373.
6. Z. H. WANG, E. M. SCHERR, A. G. MACDIARMID and A. J. EPSTEIN, *ibid.* **45** (1992) 4190.
7. N. J. PINTO, P. D. SHAH, P. K. KAHOL and B. J. McCORMICK, *Solid State Commun* **79** (1996) 1029.
8. P. PHILLIPS and H. L. WU, *J. Non-Cryst. Solids* **137–138** (1991) 927.
9. D. S. GALVAO, D. A. DOS SANTOS, B. LAK, C. P. DE MELO and M. J. CALDAS, *Phys. Rev. Lett.* **63** (1989) 786.
10. M. REGHU, Y. CAO, D. MOSES and A. J. HEEGER, *Phys. Rev. B* **47** (1993) 1758.
11. J. M. GINDER, A. F. RICHTER, A. G. MACDIARMID and A. J. EPSTEIN, *Solid State Commun.* **63** (1987) 97.
12. A. J. EPSTEIN and A. G. MACDIARMID, *Molec. Cryst. Liq. Cryst.* **160** (1988)) 165.
13. S. STAFSTROM, J. L. BREDAS, A. J. EPSTEIN, H. S. WOO, D. B. TANNER, W. S. HUANG and A. G. MACDIARMID, *Phys. Rev. Lett.* **59** (1987) 1464.
14. P. K. KAHOL, N. J. PINTO, E. J. BERNDTSSON and B. J. McCORMICK *J. Phys. Cond. Matter* **6** (1994) 5631.
15. R. SINGH, V. ARORA, R. P. TANDON, S. CHANDRA, N. KUMAR, and A. MANSINGH, *Polymer* **38** (1997) 4897.
16. M. NAKAMURA, *J. Appl. Phys.* **57** (1985) 1449.
17. F. LUX, *Polymer* **35** (1994) 2915.
18. W. S. HUANG and A. G. MACDIARMID, *ibid.* **34** (1993) 1833.
19. E. HIMADA and K. TACHIBANA, *Denki Kagaku* **62** (1994) 518.
20. N. F. MOTT and E. A. DAVIS, "Electronic Prosesses in Non-crystalline Materials" (Clarendon, Oxford, 1979).
21. R. SINGH, R. P. TANDON, G. S. SINGH and S. CHANDRA, *Philos. Mag. B* **66** (1992) 285.
22. R. SINGH, A. K. NARULA, R. P. TANDON, A. MANSINGH and S. CHANDRA, *J. Appl. Phys.* **79** (1996) 1476.
23. E. PUNKA, M. F. RUBNER, J. D. HETTINGER, J. S. BROOKS, S. T. HANNAHS, *Phys. Rev. B* **43** (1991) 9076.
24. S. KIVELSON, *ibid.* **25** (1982) 3798.
25. A. K. JONSCHER, *Thin Solid Films* **1** (1967) 213.

Received 14 January
and accepted 17 December 1997